Meeting Unmanned Air Vehicle Platform Challenges Using Oblique Wing Aircraft

Dr. R.K. Nangia
BSc, PhD, CEng, AFAIAA, FRAeS
Consulting Engineers
Nangia Aero Research Associates
WestPoint, 78-Queens Road, BRISTOL, BS8 1QX
UK

nangia@blueyonder.co.uk

ABSTRACT

There is an ever increasing emphasis on unmanned vehicles for all kinds of roles. Recent experience suggests that their capability and payoff could be complementary to manned vehicles in combat situations. However, the levels of platform and inter-disciplinary technologies need to be developed to take full advantage of their performance potential as part of an integrated defence system. This applies to all classes of Unmanned vehicles. Further, a balance has to be struck between manoeuvrability, stealth and enhancing range (persistence) whilst possibly combining reconnaissance and strike roles. A level of autonomy is implied (push button capability). Innovation and system integration is therefore called for.

Future aircraft, particularly unmanned aircraft, will have substantially "widened" flight envelopes (higher "g", AoA and ß over wider Mach, altitude and C_L ranges).

An in depth analysis of aircraft weight breakdown (structure, fuel and payload) and the trends with time, size and technology levels, together with consideration and adaptation of the Breguet Range Equation has enabled derivation of Efficiency parameters leading to an appreciation of technologies needed for innovation and for further development.

The paper focuses on the Oblique Flying Wing (OFW) concept to meet the goals of enhancing Range, Persistence whilst combining roles of Reconnaissance, Sensing and Strike. Several developing technologies, e.g. control, guidance and structure have prompted a "re-visit" to OFW. Included is a discussion of Close Formation Flying (CFF) and Air-to-Air Refuelling (AAR) as these have a very significant and favourable effect on the overall integrated military scene. A limited amount of work related to performance estimates with of L/D improvements has been shown. All this has lead to several ideas for further work and enlargement of the design space afforded by OFW.

1.0 INTRODUCTION

There is an ever increasing emphasis on the use of unmanned vehicles for all kinds of roles. Recent experience suggests that their capability and payoff could be complementary to manned vehicles in combat situations. However, the levels of platform and inter-disciplinary technologies need to be developed to take full advantage of the performance potential as part of an integrated defence system. This applies to all classes of unmanned vehicles. Further, a balance has to be struck between manoeuvrability, stealth and enhancing range (persistence), possibly combining reconnaissance and strike roles. Innovation and system integration is therefore called for. A level of autonomy is implied (push button capability).

Nangia, R.K. (2007) Meeting Unmanned Air Vehicle Platform Challenges Using Oblique Wing Aircraft. In *Platform Innovations and System Integration for Unmanned Air, Land and Sea Vehicles (AVT-SCI Joint Symposium)* (pp. 29-1 – 29-30). Meeting Proceedings RTO-MP-AVT-146, Paper 29. Neuilly-sur-Seine, France: RTO. Available from: http://www.rto.nato.int/abstracts.asp.

Future unmanned aircraft will have substantially "widened" flight envelopes (higher "g", AoA and ß over expanded Mach, altitude and C_L ranges).

Payload considerations and the Breguet Range equation enable derivation of efficiency parameters leading in turn to an appreciation of the technologies needed for innovation and for further development.

We shall focus on the Oblique Flying Wing (OFW) concept and see how this meets the goals of Enhancing Range, Persistence and combining roles of Reconnaissance, Sensing and Strike. Several developing technologies, e.g. control, guidance and structures have emphasised the need for a “re-visit” to the OFW. We include discussions on Close Formation Flying (CFF) and Air-to-Air Refuelling (AAR) as these have a very significant, favourable, effect on the overall integrated military scene.

A limited amount of work related to performance estimates with L/D improvements are shown. This leads to proposing further work in view of the enlargement of the design space associated with OFW.

2. PAYLOAD-RANGE, BREGUET RANGE & EFFICIENCY PARAMETERS

2.1 Payload Range Considerations

Fig.1 explains the various limits operating on the payload range diagram. The payload cannot be increased above the Maximum Payload limit due to structural and volume limitations. The Maximum Take-off Weight (MTOW) is also limited by structural considerations, mainly for the wing and landing gear. The Maximum Fuel volume limit is self-explanatory. It includes non-usable (residual) and reserve fuel.

Point A denotes the maximum range for the maximum payload that can be carried. Point A usually denotes the highest payload efficiency parameters for a given aircraft. For shorter ranges, the Take-Off weight (TOW) can be decreased.

In the military aircraft scene, the current trend is for stealth. To comply with stealth requirements, stores are carried internally. The carriage of stores externally will naturally increase drag and the range will usually be penalised.

Point D is the more usual prime design point with increased range over that for point A but lesser payload.

2.2 Possible Refuelling Scenarios

If an aircraft, carrying its maximum payload, were refuelled at the end of its maximum payload range (Point A), the effective range could be extended whilst still maintaining highest efficiency. Alternatively, an aircraft could take-off with maximum payload at a lighter weight (minimum fuel on board) and then refuel a little later at convenience, extending the range as required. This is more evident from the WP/MTOW sketch of **Fig.1**.

With Breguet Range Equation, following Ref.1, a series of Non-Dimensional (Non-D) Parameters arise:

Range Parameter	X = V L/D / SFC (nm)
Non-D Range (Breguet Equation)	Z = R/X = ln (W1/W2)
Fuel Burn rate	WFB/WP
Payload Range Efficiency	PRE = WP*R/WFB (nm)
Non-D Payload Range Efficiency	PRE/X

Non-D "Nangia Value Efficiency" Parameter	VEOPX = (PRE/X) /(MTOW/WP)
Non-D "Nangia Noise and Efficiency" Parameter	VEMPX = (PRE/X) /(OEW/WP)

Although the main context of the work in Ref.1 is on civil aircraft, the ideas are equally relevant to military aircraft with the emphasis on similar needs e.g. Enhancing Range, Persistence and combining roles of Reconnaissance, Sensing and Strike.

It follows that we need to:

- Increase V and L/D or reduce SFC

- Reduce drag

  Drag comprises several components.

  Peak L/D occurs when lift-induced drag is about half of the total drag.

+ Reduce Empty weight, allowing an increased payload fraction. Flying wings have low Empty fraction.

- Reducing SFC implies

  Flying near optimum propulsive conditions e.g. Mach 0.85.

On Unmanned (Combat) Air Vehicles (UAV, UCAV), AAR and CFF can be exploited to increase the range "indefinitely". This has its own brand of "features". Some aspects will be discussed.

3. OBLIQUE FLYING WINGS

3.1 Introductory Aspects

The possible advantages of Oblique Flying Wings have been appreciated for more than half a century. Dr R T Jones in the USA pioneered early work that resulted in demonstrations on the AD-1 with a pivoting wing on a fuselage-engines arrangement (Ref.2, **Fig.2**). Such a configuration was concerned more with stability and control rather than L/D issues. The presence of a fuselage and tail does not fully exploit the potential of the OFW.

In contrast to a conventional tube fuselage arrangement, the passenger compartment in a pure OFW civil aircraft design (as in BWB) is spread over a considerable spanwise fraction (mid wing). Without high levels of roll control, responsive gust and buffet alleviation and very stiff structures, the level of ride comfort will be poor for passengers seated away from the centreline.

Several Supersonic Large Flying wings were conceived, **Fig.3** and again, the main pitfalls for these early OFW designs were stability and control considerations and passenger ride comfort.

Fig.4 refers to current work emphasising supersonic flight in a demonstrator being sponsored by DARPA.

Stealth considerations lead to integrated, buried powerplants. Subsonic and Transonic designs may provide adequate thickness within the wing structure to achieve this. The very thin wings associated with Supersonic designs will provide further integration challenges.

Fig.5 summarises the perceived advantages for OFW, based on descriptions of Kroo, Ref.3. These are with regard to Wave drag, Lift-induced drag (higher Aspect Ratio) and Structure. Asymmetric flight leads to several complexities especially if sweep varies. We can add a degree of natural stealth if the planform parameters (LE and TE sweep) are chosen carefully.

It is interesting to note that the L/D of the OFW is higher than that for a corresponding swept-back wing.

The Aspect Ratio (AR) can be much higher for OFW. The wing box can be straight (no centre-line kink) and this should result in a lighter, more efficient structure. However, other issues e.g. bending and twisting need to be considered.

3.2 Adapting OFW to Unmanned Vehicles

In view of the many potentially favourable points, it appears attractive to include the OFW in the design space of unmanned vehicles. There is a difference between the concepts capable of Transonic or Supersonic speeds. It is useful to summarize the features. One obvious difference will be in the cost of developing such vehicles. Intitutively, the costs are likely to be proportional to the degree of morphing (varying sweep) as well as maximum speed capability. The situation is relatively "fluid". The capabilities of OFW are not yet sufficiently understood to determine how far the flight envelopes could be developed. An "iterative" development approach is needed.

Transonic Concept

From the SFC viewpoint, it is desirable to fly at high transonic speeds near 0.85 (e.g. Ref.4). In general, higher cruise speeds require increased sweep and thinner wings. Relatively low sweep and small chords, encourage the retention of laminar flow (highly dependent upon the vehicle size).

If we can confine the configuration to a fixed sweep layout (about 30 deg.), then the intake and nozzles may not require pivoting or deflection. However, moderate sweep changes may be still be possible +/- 5 deg sweep (10 deg total) whilst matching of the inlet and nozzle units could be achieved with local deflections of say +/- 5 deg, well within the usual variations available.

For OFW, speed variation (take-off and landing to cruise) implies complex stability and control (S & C) issues. Sweep changes will further complicate the matter. Conventional TE controls may not be adequate. Morphing wing structures and tip deflection may provide suitable answers. For example, the movement of the neutral point with increasing Mach number can be controlled with small local changes in tip fold and twist (morphing).

The aerofoil shapes need to be thick for fuel and payload carriage. We anticipate t/c of the order of 12-14% streamwise at 35 deg sweep ("middle" wing) with 15-17% on the "forward" wing portion. With high L/D and the possibility of exploiting AAR, fuel capacity needs are modest. This leads to payload benefits.

The low-speed near-field performance is more akin to that of a (very) high AR wing glider in "asymmetric" flight. Take-off and landing phases are challenging.

The design aspects are covered in Section 4.

Supersonic Concepts – Using Variable Sweep

Whilst having much in common with the Transonics, Supersonic flight implies variation to higher sweep (60+ deg.) and lower t/c (of the order of 6% streamwise for Mach 1.4). We consider the effects of sweep on a typical wing planform shape. At zero sweep, low speed, the wing has AR=12.0 and streamwise t/c=15.0%. At 30^{o}, 60^{o} sweep the wing has effective AR of 8.11, 3.31 and t/c of 13.0%, 7.5% respectively.

A highly swept configuration, designed for supersonic flight, will naturally have poor low speed capability. Reducing the sweep as speed decreases from supersonic through transonic to low speed to overcome this obviously adds a degree of complexity to the propulsion aspect. Modest sweep changes for

transonic to low speed variation could be accommodated by simple nozzle deflection. Changes in sweep of the order of 60^o to 30^o will have a significant bearing on intake and nozzle design and performance and any stealth requirements for the configuration.

These varied considerations, when taken in conjunction with fundamental issues such as fuel and payload accommodation, structures, aero-elasicity, stability and control, etc., lead to a challenging design problem.

A research programme, "Switchblade" (Ref.12), is being conducted in the USA under DARPA sponsorship. With varying sweep, Switchblade can achieve a wide and efficient subsonic-supersonic flight envelope capability. An unmanned flying demonstrator is being planned by Northrop-Grumman in consultation with AFRL. The programme remains very challenging in view of the need to balance the asymmetric forces and moments, stability levels and aero-elastic implications (e.g. Refs.5-5.5).

3.3 Range Enhancement, Autonomy & Operations

With the on-going development of autonomy for unmanned systems, we can include:

Close Formation Flying (CFF)

There are many interesting aspects that apply to the transonic and supersonic concepts. Benefits of 30% - 50% reductions in lift-induced drag are feasible in tightly controlled formations of two vehicles. Some of these aspects are addressed in Refs.5-12. With multiple vehicles (more than two), the gains are further amplified. For example, five vehicles may lead to 80% reduction in lift-induced drag. All this implies a sizeable and favourable impact on extending ranges. Many details are involved and need to be studied. Section 5 deals with our current work.

Air to Air Refuelling (AAR)

The adoption of AAR is assumed in military aircraft. Nearly all current and future combat and transport aircraft have AAR capability. This allows aircraft to be smaller than would be required to carry out similar operations without AAR. The range extension can be infinite. Restrictions associated with manned flight are not applicable to unmanned vehicles. The ratio of Payload to MTOW can be increased very significantly. There are significant control problems to be addressed. Section 6 provides more detail.

4. OBLIQUE FLYING WING DESIGN ASPECTS – TRANSONIC CONCEPT

There are a series of design compromises that will be needed when designing a transonic OFW. A challenging and interesting programme arises.

For our initial studies (Ref.12), we have chosen a planform (AR = 7.576) with LE sweep 30 deg., **Fig.6**, based on notional, unclassified, pictorial concepts discussed in various recent publications (e.g. Ref.13).

We can now show a specimen set of results that go some way towards giving an amount of credibility to the ideas promulgated. These will also illustrate the design capability that has been developed.

4.1 Basic Oblique Wing Design

Following Refs.12, 14-15, the wing is initially assessed in its planar, no camber, state. The wing is then designed for a known C_L and Mach combination. At present, simple aerofoil sections have been used. The design process being staged, gives a feel for what is happening in terms of camber and pressure distribution development and Centre of Pressure location.

Results for the planar (non-cambered) 30° LE swept OFW at Mach 0.8 are shown in **Fig.7(a-d)**. The planform and surface thickness distribution are shown in **Fig.7(c)**. $C_L - \alpha$ and $C_m - C_L$ variations are shown in **Fig.7(a)**, C_m about the Mach 0.8 aero center, with spanwise load distributions in **Fig.7(b)**. The lift curve slope is 0.101/°, giving $C_L = 0.303$ at 3.0° incidence. The chordwise Cp distributions of **Fig.7(d)** are typically "peaky" for the undesigned case, especially at the rearmost, right tip. This establishes the design problem. We select a design C_L of 0.3 at Mach 0.8. In general, we may then choose to design for minimum drag (elliptic loading), a pre-determined level of stability or a compromise between the two, or indeed a structural Bending Moment (BM) constraint.

Fig.8(a-f) refers to a design for C_L=0.3 at Mach 0.8 with an elliptic spanwise loading (minimum drag) target. Note from the spanwise loadings **Fig.8(a)** and the chordwise Cp distributions **Fig.8(d)** that the target distribution has been achieved within five design cycles. The Cp distributions, Cp – x and Cp – x/c from a Panel method, **Fig.8(c)** and Cp contours from an Euler method (Ref.16) evaluation, **Fig.8(d)** compare well, as envisaged. The spanwise loadings show a small region of suction force (negative C_{Di}) at the right, trailing, tip. The resultant camber distribution **Fig.8(b)** is smooth and consistent. The camber profile is positive, without inflection, with 4.10° twist at the left tip and 0.16° twist at the right tip.

The $C_L - \alpha$ and $C_m - C_L$ relationships for the design case (compared with those for the non-cambered OFW) are shown in **Fig.8(f)**. C_m is referenced about the Mach 0.8 neutral point. Both the non-cambered and designed OFW are stable with a C_{mo} offset induced by the camber design. The design process easily accommodates stability requirements if required.

Fig.8(e) shows the relaxed wake for the isolated OFW at design conditions. At the design point, there is no appreciable change in C_L due to wake relaxation. C_m is slightly more negative (–0.0096 cf –0.0087). It is useful to appreciate that the wake, overall, drifts downwards. The edge of the wake, tip region, rolls upwards. With side-slip the wake shape will change.

The effects of the lead aircraft wake on a trailing aircraft need to be considered in formation flying. An indication of the affects can be deduced from calculations with rigid trailing wakes but more realistic, overall effects need to be assessed with fully relaxed wakes (Section 5).

4.2 Oblique Flying Wing with 75° Folded Tip / Winglet, Mach 0.8, $C_L = 0.3$

Fig.9 (a-e) refers to an OFW flying at 30° sweep with 75° folded tip or winglet, Ref.14. This also acts as a vertical fin or as a control (deflection capability). The first problem is to see what its cambered shape would be when designed for particular conditions. The target as before, was simple "optimum" minimum drag loading from Trefftz-plane basis. There is no C_{LL} constraint. The spanwise loadings, for the first and fifth cycles, with target, are shown in **(a)** and **(b)** and are presented in the unfolded sense.

Within five cycles, a reasonable camber surface developed **(c)** for this, rather unique, design problem. The resultant Cp-x distributions **(e)** at the design condition are well behaved. The distributions on the winglet are slightly more "peaky" than elsewhere. Stability and control analysis for this case will be interesting and well within the capabilities of the technique. This provides an additional yaw and sideslip challenge.

5. CLOSE FORMATION FLYING (CFF) EXAMPLES

The physics behind CFF is based on the downwash and upwash characteristics behind an aircraft wing, **Fig.10.** The upwash field generated by a lead aircraft can be used to advantage by a trailing aircraft. The idea extends to multiple aircraft arrangements.

The cruise drag of an aircraft comprises several components, Ref.16, **Fig.11**. The major components are: Friction (48%) and Lift-Induced (35%). This is subject to interference effects in close aircraft formations.

Using a simple horse-shoe vortex model, Blake and Multhopp (Ref.5) have published an interesting graph on lift-induced drag variation as a function of the relative (lateral) positions between a lead and a trail aircraft both of the same size, **Fig.12**. Although subject to chordwise location effects, this shows that the "sweet spot" for a drag reduction of 50% occurs at 22% span overlap with the wings at the same altitude. The ability to fly accurately to maintain lateral position is crucial. Half of the drag benefit is lost, if the lateral/vertical position cannot be maintained to better than 10% of wing span.

5.1 Formation Layouts

Formation Layouts & Geometry

Various formations and core configurations are shown in **Figs.13 & 14**. We consider formations using identical (planform and sweep sense) equi-sized aircraft. In particular, we assess Core 1 and Core 2 geometries. The formation spacing parameters dx/b, dy/b and dz/b are defined in terms of the Trail aircraft geometry, as shown for Core 1 geometry in **Fig.15**. The origin corresponds to the Trail aircraft apex (x_o) and left tip (y_o). This scheme allows spanwise overlap to be represented by a positive value. The streamwise spacing parameter, dx/b, is defined as the distance from the Lead aircraft tip TE to the Trail aircraft tip LE for the in-line tips at dy/b=0.0. Note the significant difference between Core 1 and Core 2 formations. In **Fig.15**, the wings are depicted at dx/b = 1.0 and both dy/b and dz/b at 0%. The Trail aircraft wing tip is also shown at dy/b = 30%, dz/b = 30%.

For simplicity, we have mainly used planar wakes. However, some cases include relaxed wakes. Cross-wind effects have not been included in this paper. Provided most of the Trail aircraft wing remains outside the wing wake edge of the Lead aircraft, the former experiences a favourable upwash asymmetric field.

If we assume that the basic aircraft is a near-optimum configuration (isolated flight), then the task is to focus on the changes in geometry required (e.g. by camber, twist or controls) on the Trail aircraft, cancelling the induced field effects e.g. total lift, rolling moments, as far as possible. We have focussed on Core 1 and 2 formations initially before assessing Core 3 and 4 formations.

The Lead aircraft has been assumed to be reasonably far upstream (dx/b = 1.0) and this has relatively small induced effects due to formation flight (of the order of less than 1 drag count in C_{Di} and less than 0.3% in C_L). It is appreciated this may not be the case for other configurations in formation. The scope of the assessments can be extended as needed.

Initially we establish the induced effects on the Trail aircraft by varying lateral and vertical displacements. We have selected cases of interest with significant drag reductions and have then re-designed the Trail aircraft wing to eliminate the additional lift and rolling moment induced. The Trail aircraft is then considered to be in a trimmed state.

5.2 CORE 1 Formation

Planar Wakes

As the Trail aircraft positions itself behind the Lead aircraft (y and z translations), it experiences changes in C_L and C_{Di}. These changes are shown as ΔC_L% and ΔC_{Di}% vectors, based on the isolated designed aircraft values, in **Fig.16(a-b)**. The vector origins illustrate the physical displacement of the Trail aircraft left tip in the y-z plane. Note, at dy/b=dz/b=0 the Trail aircraft left tip is in-line with the Lead aircraft right tip. Increase in C_L is plotted horizontally to the right. Decrease in C_{Di} is plotted vertically upwards. Beneficial locations (positive ΔC_L% and negative ΔC_{Di}%) are indicated by vectors to the right and upwards. The Trail tip loci for constant ΔC_L of –10%, -5%, 0%, +5% and +10% are shown in **Fig.16a)**. We can immediately infer that the region near the Lead aircraft right tip, centred at about 10% span (b)

overlap is of most interest. **Fig.16(b)** shows this region in more detail. Two displacements were selected for re-design (trimming) of the Trail aircraft, 2.5% and 5.0% b overlap with the Trail aircraft 2.5% b below the Lead aircraft.

At dy/b = 2.5%, dz/b = -2.5%, before re-designing the Trail aircraft, the benefits are ΔC_L = 13.6% and ΔC_{Di}% = -22.4%. After re-designing ΔC_{Di} = -33.5% and ΔC_L is less than 1%. Slightly greater benefits are achieved at dy/b = 5.0%. Before re-design ΔC_{Di} = -23.3% and ΔC_L = 13.9%. After re-design ΔC_{Di} = -35.0% and ΔC_L is less than 1.0%. The vectors for the re-designed (trimmed) cases are plotted as dashed lines in **Fig.12(b)** and can be seen as solid, near vertical lines in **Fig.16(a)**.

The additional wing twist required as a result of re-designing is shown in **Fig.17**. Negative values indicate that the re-designed OFW has its local twist reduced to eliminate the additional lift induced. As expected this is concentrated near the tip and is less than 1^o. The possibility of using variable camber to achieve these changes exists.

We now discuss the effects induced on the Trail aircraft for one formation location.

For dx/b = -1.0, dy/b = 2.5%, dz/b = -2.5%, **Fig.18(a)** shows the spanwise loadings on the trail aircraft in formation and those for the aircraft in isolation. The additional lift induced is dominant at the spanwise location directly behind the lead aircraft tip (inducing roll) but is also distributed over the entire span. The drag reduction is also evident. Cp distributions are shown in **Fig.18(c)**. The changes in Cp distribution may be deduced by comparing **Fig.8(c)** and **Fig.18(c)**. The resulting increase in C_L and reduction in C_{Di} were 13.6% and –22.4% respectively, **Fig.15**.

The spanwise loadings after three re-design iterations to trim the Trail aircraft are compared with the isolated, design case in **Fig.18(b)**. Cp distributions for the redesigned case are shown in **Fig.18(d)**. The redesigned cambered and twisted surfaces are compared with the original isolated datum wing in **Fig.18(e)**. This gives an indication of the changes needed on the trail aircraft geometry to cancel the induced effects due to formation flight. The additional twist is shown in **Fig.17**. After re-design ΔC_{Di}=-35.0% and ΔC_L is less than 1.0%.

Relaxed Wakes

A typical Lead aircraft relaxed wake geometry for the Core 1 formation is shown in **Fig.19**. The additional effects on the Trail aircraft due to Lead aircraft wake relaxation are small for this type of formation. For displacement dy/b=2.5%, dz/b=-2.5%, benefits in lift and drag are 13.7% and –22.6% respectively, compared with 13.6% and –22.4% with planar wakes.

Euler results , dx/b=-1.0, dy/b=2.5%, dz/b=-2.5%

For comparison, Euler calculations were conducted on selected cases. These have the benefit of implied wake relaxation. For both Lead and Trail aircraft in their basic design state, Mach and Cp contours on the Trail aircraft in Core 1 formation at dy/b=2.5%, dz/b=-2.5% are shown in **Fig.20**. The Lead aircraft contours may be regarded as the design condition. Note that the Trail aircraft exhibits more extensive low Cp regions. The Cp distributions compare well with the Panel method results (**Fig.18(d)**). Mach and Cp contours on the Trail aircraft after re-designing (trimming) are shown in **Fig.21**. Now the contours on Lead and Trail aircraft are almost identical.

5.3 Core 2 Formation

Relaxed Wakes

A typical Lead aircraft relaxed wake geometry for the Core 2 formation is shown in **Fig.22**. For displacement dy/b=2.5%, dz/b=-2.5%, benefits in lift and drag are 11.1% and –20.9% respectively, compared with 12.1% and –22.8% with planar wakes. As for the Core 1 example, although small, the effect of relaxing the Lead aircraft trailing wake has reduced the benefits on the Trail aircraft for this case.

Euler results , dx/b=-1.0, dy/b=2.5%, dz/b=-2.5%

As for Core 1, Euler calculations were conducted on selected cases. For both Lead and Trail aircraft in their basic design state, Mach and Cp contours on the Trail aircraft in Core 2 formation at dy/b=2.5%, dz/b=-2.5% are shown in **Fig.23**. The Lead aircraft contours may be regarded as the design condition. Note that the Trail aircraft exhibits more extensive low Cp regions. Mach and Cp contours on the Trail aircraft after re-designing (trimming) are shown in **Fig.24**. Now the contours on Lead and Trail aircraft are almost identical. The Euler evaluations confirm the trends established from the Panel method results.

5.4 Core 3 and Core 4

We have made a brief assessment of the benefits gained by the Trail aircraft in Core 3 and Core 4 formations for the same comparative displacements, dy/b = 0% (tips in line) and dz/b = -2.5%. In Core 3, a single Trail aircraft follows two Lead aircraft. In Core 4, two Trail aircraft follow a single Lead aircraft. **Fig.25** shows the ΔC_L% and ΔC_{Di}% vectors for Trail aircraft in Core 1, Core 2, Core 3 and Core 4 formations. The sign convention is the same as that used in **Figs.12 & 19**.

For Core 3, effectively, the benefits gained by the single Trail aircraft (solid line vector) are the additions of those on the Trail aircraft in the Core 1 and Core 2 formations (dashed line). The results are very similar. For Core 4, the two Trail aircraft (Left and Right) each benefit from a single Lead aircraft. In this case, the addition of the benefits gained by the two Trail aircraft (dashed line) is again very similar to the additions of the Core 1 and 2 Trail aircraft benefits.

We may deduce that the Trail aircraft benefits for multiple aircraft in formation are, to a first order, cumulative. However, this may not be true for other formation layouts.

It is anticipated that as the Lead aircraft move closer together (decreasing dy) in Core 3 formation, the interaction between the trailing wakes will become more dominant and the effects on the Trail aircraft will not be simple summations. As the Trail aircraft move closer together in Core 4, the forward effect on the Lead aircraft may intensify and a mutual interference between the Trail aircraft may also result. The interaction effects are likely to be complex and the benefits may not be simple summations. In all cases, the streamwise spacing of the aircraft will also have a significant effect.

5.5 Some Comparisons and Inferences

Prior to any redesign of the Trail wing to eliminate induced Rolling moment, we look initially at the primary benefits gained for each formation. We have presented ΔC_L% and ΔC_{Di}% (Lift and Induced Drag increments) as vectors in **Fig.16**, for Core 1. The scalar length of these vectors, ΔC_{VM} (vector addition of ΔC_L% and ΔC_{Di}%), gives an indication of the possible ΔC_{Di} benefits that may occur after redesigning the Trail wing to eliminate the additional Lift and Rolling moment. Only regions in the y-z plane where ΔC_L is positive and ΔC_{Di} is negative are considered. The variation of ΔC_{VM} with span overlap is shown in **Fig.26** as solid lines, for Core 1 and Core 2 formations (dz/b = 0%, -2.5% and –5.0%). The ΔC_{Di} levels (ΔC_{VM} where the ΔC_L component is reduced to zero) after redesigning are shown as dashed lines for dz/b = -2.5%. Note that for Core 1, increasing positive overlap implies that the Trail aircraft moves from right

to left behind the lead aircraft, whereas for Core 2 the Trail aircraft will be moving from left to right. From extremely limited data so far, it may be concluded that the Core 1 formation offers marginally higher benefits in terms of Induced Drag reduction.

Comparing Core 1 and Core 2 formations at dy/b = 0% (opposing tips in-line), as the Trail aircraft sinks from dz/b = 0% to 5% below the Lead aircraft, ΔC_L decreases from +15% to +11% for Core 1 and from 12% to 10% for Core 2. Similarly the Induced Drag benefits decrease from ΔC_{Di} = -27% to –18% for Core 1 and from –24% to –18% for Core 2. On this basis, Core 1 formation again, has a slight advantage over Core 2. However, this comparison is made for a particular OFW design (not optimised), with Lead and Trail aircraft at a given x displacement, in an inviscid flow field with a Lead aircraft rigid trailing wake. More work needs to be carried out to define a suitable OFW geometry and then to assess the implications of wake relaxation and formation configurations (dx, dy and dz displacements).

For selected cases, we have derived the wing twist required, **Fig.17**, to cancel the formation induced rolling moment. This is a useful measure for evaluating variable camber deflections that may be called for.

After redesign iterations, the incremental roll and pitching moment effects, due to formation flying, are small. Any yawing moment effects can be compensated for by differential thrust on aircraft with twin or more engines. This may be more preferable than using rudder and aileron deflection. Such considerations begin to fall under optimum control aspects.

For the complete trail aircraft configuration, including other contributions to drag (nacelles, viscosity, trim) we arrive at a total drag coefficient, C_D (= C_{Di} + C_{Do} and trim contribution). The ΔC_{Di} values will need to be factored by about 40% to give an estimate of the overall drag benefits. Such estimates will need confirmation with more detailed studies. Nevertheless, it is estimated that ΔC_D of 15-20% appear possible from the few locations studied so far. The underlying design method shows considerable potential for being utilized in studies including the use of Euler and Navier Stokes solvers as needed.

6. AAR FORMATION CONSIDERATIONS

The operation and control of aircraft during AAR formation flight is a vast subject in itself. Add to this the possible autonomy of individual aircraft within an AAR formation and interesting complexities arise. We can note a few important points with reference to refuelling locations and areas of research.

Note from **Fig.12** that in the symmetric refuelling formation (0% lateral spacing), a drag penalty appears depending strongly upon vertical separation (50% span vertical spacing: penalty 25% and at 25% span vertical spacing: penalty rises to near 50%). The 0% penalty line corresponds to about 40% overlap of wings (at 0% and more vertical spacing). We confirm that some refuelling locations will be better.

The drag changes are accompanied by interference effects e.g. in pitch, roll and yaw. In our recent work we have analysed such formation aspects, with more detailed flow models, including aircraft size differences (Refs.11 - 12). Such considerations will be important in practical operational terms.

The thrust produced by a jet engine reduces as altitude increases. With high by-pass engines, this can be more marked. With 0% lateral spacing, the drag penalty experienced by the trail aircraft requires a significant increase in thrust for the duration of the tanking operation. At certain altitudes, the required increase in thrust may not be available and the tanking procedure has to be carried out at lower altitude. This problem reduces as the 0% drag penalty curve is approached.

All this indicates the need for size effects in formations to be understood. An unmanned vehicle could be smaller than the tanker and the favourable effects of formation may be small. In the approach to a formation, control effects need to ensure a “naturally” stable situation.

7. LIFT, DRAG & PERFORMANCE ESTIMATIONS

The overall contributions to total drag C_D (= C_{Di} + C_{Do} and trim contribution) were initially discussed in Section 5. Keeping C_{Do} within desirable limits and also its initial evaluation are notoriously difficult. Estimates of total drag breakdown for arbitrary C_L=0.2 and 0.4 designs, with varying C_{Do} levels (0.016 to 0.024), are shown in **Fig.27**. Lift induced drag (C_{Di}) has been estimated for each case at the design condition. To this is added a skin friction term (C_{DoSF}) and a further zero lift drag term ($C_{DoOTHER}$) attributable to intakes, etc. The corresponding L/D achieved are indicated. **Fig.28** shows the variation of L/D for the two design cases (C_L=0.2 and 0.4) with a similar range of C_{Do} values. For UAV and UCAV configurations, L/D in the region of 15 - 20 may be typical. The OFW may offer a lower C_{Do} than conventional wing plus fuselage configurations and hence achieve L/D at the higher end of this range. With Formation flying, we should be able to extend the L/D curves to 20-25 or beyond.

The Breguet Range Equation (Section 2 and Ref.18) for the Equivalent Still Air Range (ESAR) is:

$$ESAR = L/D * V/SFC * \ln(W1/W2)$$

Where W1 and W2 are the initial and final aircraft weights (difference being the fuel consumed), V is the aircraft speed (kt) and sfc is the specific fuel consumption (lb/hr/lb). W1 is the Take-off weight (TOW) and comprises Operating Empty weight (OEW), Payload (WP) and total Fuel (WF). The resulting value of ESAR assumes that all the fuel is consumed. A proportion of the ESAR may be reserved for contingencies, e.g. ground manoeuvres, headwinds, diversions, etc. Typically ESAR = 500 + 1.06 x Range (nm), i.e. 500 nm and 6% of the Range are reserved for contingencies (Reserve Fuel). For detailed performance estimations, further modifications to the Breguet Range Equation will be necessary to allow for variations in L/D during climb and descent, acceleration / deceleration phases, variations in sfc, etc.

We show the variation in TOW with Endurance (hr) and Range (nm) for a range of L/D values in **Fig.29** assuming OEW/TOW = 0.50, V = 460 kt (Mach 0.8) and WP = 5000 lb for sfc = 0.9 and 1.0.

For simplicity, fuel allowances for contingencies have not been made and the Endurance is based on the full fuel load.

For an Endurance of just under 10 hr, L/D would need to be over 20 (very low C_{Do}) and sfc = 0.9 and the resulting UAV would have TOW = 50,000 lb. Using more advanced materials in the construction might reduce OEW/TOW to 0.5. A UAV with TOW = 40,000 lb, less efficient engines (sfc = 1.0) would also have an Endurance of just under 10 hr, **Fig.30**.

This type of TOW – Range diagram illustrates the “trade-offs” that can be used to achieve a certain Range or Endurance. The importance of achieving high L/D is evident. The reductions in C_{Di} experienced by the Trail aircraft in CFF were estimated to give a ΔC_D of about 15%. An L/D of 20 would therefore increase to 23.5. Using this type of estimate and data such as in Fig.29 we can derive a new endurance or Range for aircraft in CFF.

8. CONCLUDING REMARKS & GENERAL INFERENCES

There is an ever increasing emphasis on unmanned vehicles for all kinds of roles. Recent experience suggests that their capability and payoff could be complementary to manned vehicles in combat situations. However, the levels of platform and inter-disciplinary technologies need to be developed to take full advantage of their performance potential as part of an integrated defence system. This applies to all classes of unmanned vehicles. Further, a balance has to be struck with manoeuvrability, stealth and enhancing range (persistence), possibly combining reconnaissance and strike roles. Innovation and system integration is therefore called for. A level of autonomy is implied (push button capability).

Future unmanned aircraft will therefore have substantially "widened" flight envelopes (higher "g", AoA and ß over Mach, altitude and C_L ranges).

In this paper, we began with Payload considerations and the Breguet Range Equation which enabled the derivation of Efficiency parameters. In turn these led to an appreciation of technologies available and those needed for innovation and for further development.

We focussed on the OFW concept to show how this can meet the goals of enhancing Range, Persistence and combining roles of Reconnaissance, Sensing and Strike. Several developing technologies, e.g. control, guidance and structures have emphasised the need for a “re-visit” to OFW. Design aspects of OFW for transonic speeds have been demonstrated. The emphasis has been on a cost-effective moderately swept configuration with limited morphing abilities. There is potential for large L/D values touching 15-20.

We have included a discussion on Close Formation Flying (CFF) and Air-to-Air Refuelling (AAR) as these have a very significant and favourable effect on the overall integrated military scene.

With OFW, several different types of “handed” formations arise. We have described typical two-aircraft formations with potential lift-induced drag savings of 15-20% or more. The savings will increase with multiple aircraft formations. The drag savings translate directly into range enhancement. Several possibilities exist for further work taking into account, operational issues such as control, off-design performance and practical implementation.

A limited amount of work, related to performance estimates with effect of L/D improvements, has been shown. This needs to be expanded with comparisons against more “conventional” layouts.

The work carried out so far has led to a confidence in the design methods. The whole process is enlightening as it gives, at every stage, a physical feel for various parameters particularly stability and control. An indication of versatility has been given both within individual design schemes and the scope of geometries accommodated.

9. POSSIBLE FUTURE WORK

Several avenues for future work have arisen in view of the enlargement of design space with OFW.

The techniques used on OFW design and evaluation may require further development and validation against other approaches. The method needs to be assessed more extensively with other “core” solvers. The capability of the method to design for a given spanwise loading, linked to stability levels has been encouraging. This needs to be extended to other design targets such as shock location control, TE controls etc. Design in the presence of engines and attached “non-lifting” bodies needs to be explored. A list of avenues to follow is:

- Different planform geometries for OFW as well as packaging issues.
- Performance studies to establish baseline with OFW for different sizes.
- Focus on flight envelopes and packaging capabilities.
- Control of forces and moments
    - So far only Lift and Rolling Moment attempted, other details needed.
- Induced-Drag reductions relative to total Drag.
- Understanding of camber/twist – vari-cam or other systems
- Including wing-tip morphings
- Formation positioning changes, relative size effects

- Sideslip effects
- Verification with higher order codes.
- Performance figures
- Operational realities, unsteadiness of wakes

It will be interesting to further extend the knowledge, applying the method to multiple aircraft type formations, including mixtures of conventional wing-fuselage, delta wing and future types such as Blended Wing Bodies including of course Oblique Wings.

ACKNOWLEDGEMENTS

The author has pleasure in acknowledging technical help of Dr. M. E. Palmer. The work is a part of in-house R & D activities. Opportunities for collaboration are warmly invited. Any opinions are the author's.

REFERENCES

1. NANGIA, R.K.., "Commercial Aircraft Efficiency Parameters", RAeS Aeronautical Journal, August 2006.

2. NASA Dryden Website.

3. KROO, I., "Desktop Aeronautics", www.

4. GREEN, J.E., RAeS Aeronautical Journal, August 2006.

5. BLAKE, W. and MULTHOPP, D, "Design, performance and modelling considerations for close formation flight",. AIAA Paper 98-4343 (1998).

6. SOBIECZKY, H., "Manual Aerodynamic Optimisation of Oblique flying Wing, ICAS-98-1.1.3, 1998.

7. HAGENAUER, B. "NASA Studies Wingtip Vortices." Aerospace Engineering Online: Technology Update, Jan/Feb 02, http://www.sae.org/aeromag/techupdate/02-2002/page5.htm.

8. IANNOTTA, B. "Vortex Draws Flight Research Forward." Aerospace America, Mar 02, 26-30.

9. RAY, R. J., et al. "Flight Test Techniques Used to Evaluate Performance Benefits During Formation Flight." AIAA paper 2002-4492, Monterey CA, Aug 02.

10. WAGNER, G., Jacques, D., Blake, W. and Pachter, M., "Flight Test Results of Close Formation Flight for Fuel Savings." AIAA paper 2002-4490, Monterey CA, Aug 02.

11. NANGIA, R.K., PALMER, M.E, "Formation Flying of Commercial Aircraft – Controlling Induced Effects, Variation in Relative Aircraft Size / Spacing", Proposed Paper for 2007.

12. NANGIA, R.K., PALMER, M.E., "Formation Flying of Oblique Wing Aircraft, Assessment of Variations in Formation Configuration – Induced Effects & Control", Paper for 2007.

13. "DARPA sponsored Oblique Wings" Flight International, 13-19 September, 2005.

14. NANGIA, R.K., PALMER, M.E. & DOE, R.H., " Aerodynamic Design Studies of Conventional & Unconventional Wings with winglets", AIAA-2006-3460. 25th Applied Aero Conference, San Francisco, June 2006.

15. NANGIA, R.K., PALMER, M.E., "Morphing UCAV wings, Incorporating in-Plane & Fold-Tip Types – Aerodynamic Design Studies", AIAA-2006-2835. 25th Applied Aero Conference, San Francisco, June 2006.

16. GUPTA, K.K. & MEEK, J.L., "Finite Element Multidisciplinary Analysis", AIAA.

17. GREEN, J.E., "Greener by Design – the Technology Challenge", The RAeS Aero. Jo., Vol.106, No.1056, February 2002, Erratum, Vol 109, no 1092. Feb 2005.

18. JENKINSON et al, "Civil Jet Aircraft Design", Arnold, 1999.

NOMENCLATURE

AAR	Air-to-Air Refuelling
AR	Aspect Rato tio
BWB	Blended Wing Body
b	= 2 s, Wing span
c	Local Wing Chord
c_{av}	= c_{ref} = S/b, Mean Geometric Chord
C_A	= Axial force/(q S), Axial Force Coefficient
C_{AL}	Local Axial Force Coefficient
C_D	= Drag Force /(q S), Drag Coefficient (C_{Di}+ C_{D0})
C_{Di}	Lift Induced Drag Coefficient
C_{DL}	Local Drag Coefficient
CFF	Close Formation Flying
CG	Centre of Gravity
C_L	= Lift Force/(q S), Lift Coefficient
C_{LL}	Local Lift Coefficient
C_m	= m/(q S c_{av}), Pitching Moment Coefficient
C_{mL}	Local Pitching Moment Coefficient
C_P	Coefficient of Pressure
ΔC_L	Difference in C_L
ΔC_{Di}	Difference in C_{Di}
ΔC_{VM}	Magnitude of the vector addition of □C_L and □C_{Di}
dx, dy, dz	for specifying formation relative distances
LE, TE	Leading Edge, Trailing Edge
LEF, TEF	Leading Edge Flap, Trailing Edge Flap
L/D	Lift to Drag ratio
m	Pitching moment
M	Mach Number
MTOW	Maximum Take Off Weight
OEW	Operating Empty Weight
OFW	Oblique Flying Wing
PRE	Payload Range Efficiency (PRE / X Non-dimensional)
q	= 0.5 ρ V^2, Dynamic Pressure
R	Range (nm)
RBM	Root Bending Moment (typically of wing about fuselage side)
Re	Reynolds Number, based on c_{av}
s, S	semi-span, Wing Area
S_L	Lead aircraft Wing Area

S_T	Trail Aircraft Wing Area
SFC	Specific Fuel Consumption
V	Free-stream Velocity
VEOPX	Non-dimensional “Nangia Value Efficiency” Parameter
VEMPX	Non-dimensional “Nangia Noise and Efficiency” Parameter
W1, W2	Initial and Final aircraft Weights
WP	Weight of Payload
WFB	Block Fuel
X	Range Parameter (V L/D / SFC)
x, y, z	Axes system of an aircraft
x_{AC}	Chordwise position of Aerodynamic Centre
x_{CP}	Chordwise location of Centre of Pressure
y_{CP}	Spanwise location of Centre of Pressure
Z	Non-dimensional Range (R / X)
α	AoA, Angle of Attack
ß	$\sqrt{(1-M^2)}$
λ	Taper Ratio, c_t/c_r
Λ	LE Sweep Angle
η	= y/s, Non-dimensional spanwise distance
ρ	Air Density

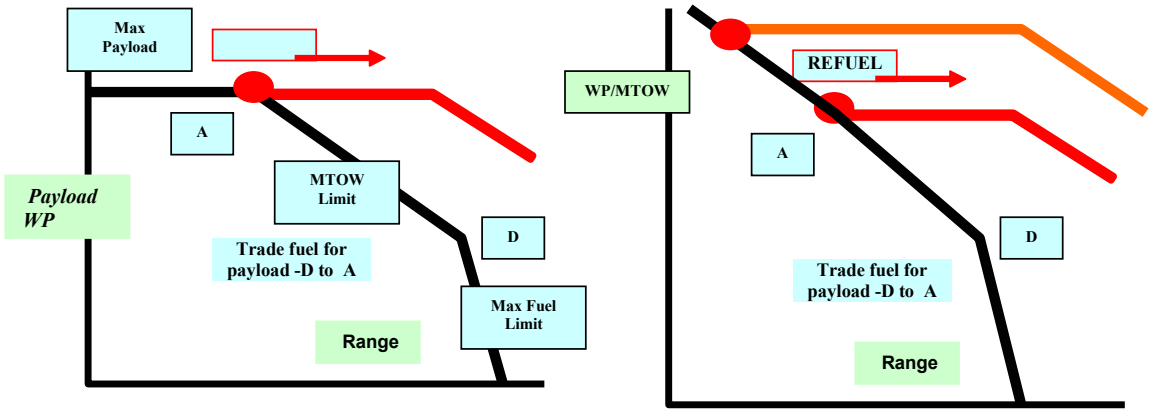

In Terms of WP

In Terms of WP / MTOW

FIG.1 RELATING Various Limits in the Payload-Range Diagrams

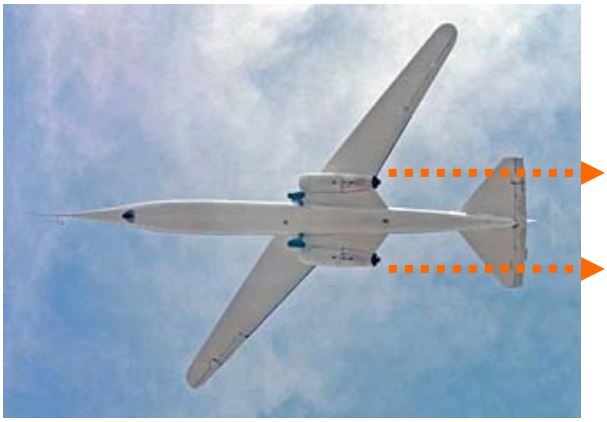

FIG.2 NASA AD-1, PIONEERED BY R T JONES

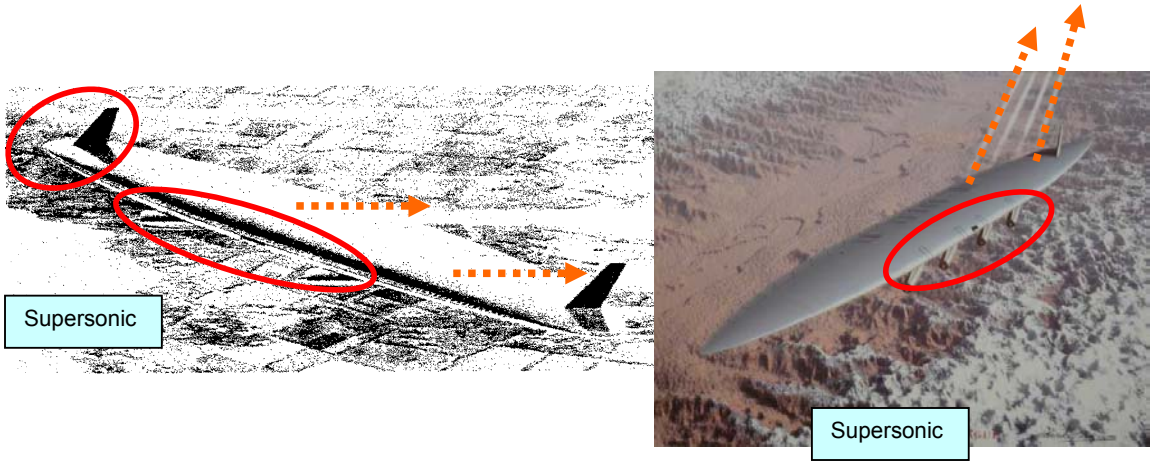

FIG.3 LARGE SUPERSONIC OBLIQUE WINGS

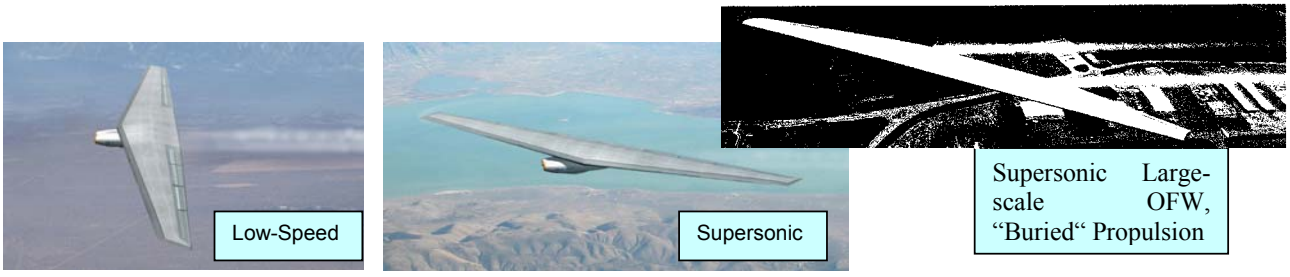

Fig. 4 OBLIQUE FLYING WINGS, OFW (DARPA)

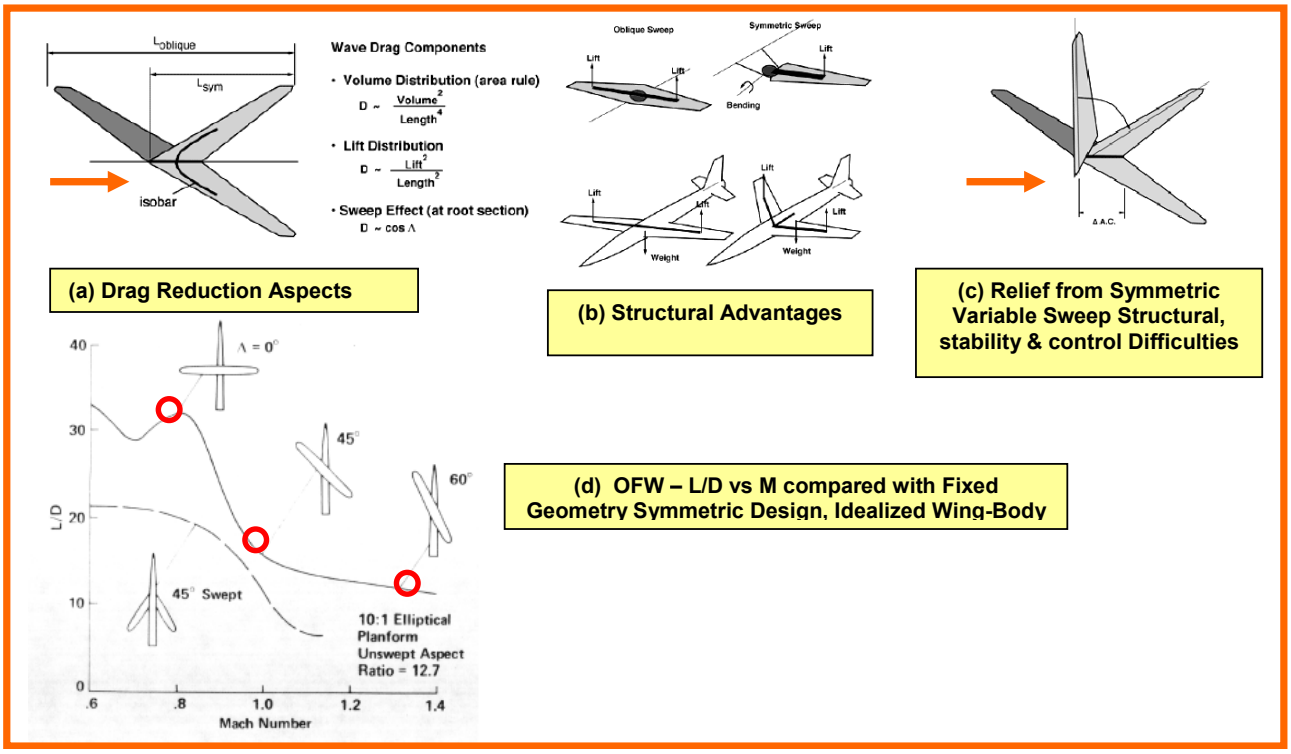

Fig. 5 OBLIQUE FLYING WINGS, SOME POSSIBLE PERCEIVED ADVANTAGES

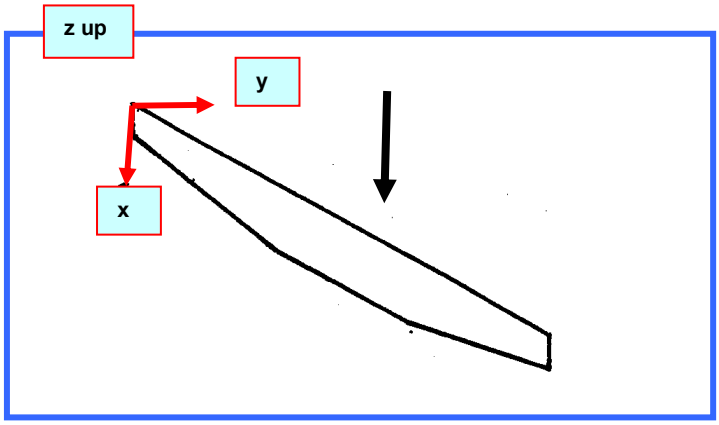

Fig. 6 OBLIQUE FLYING WINGS, PLAN GEOMETRY ASSUMED, 30 deg. LE SWEEP

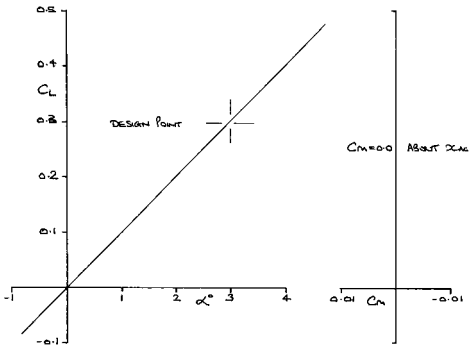

(a) Lift & Pitching Moment

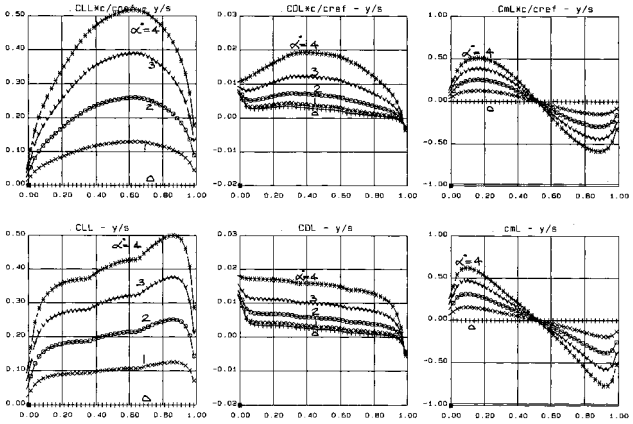

(b) Spanwise Loadings For AoA 0 – 4 deg.

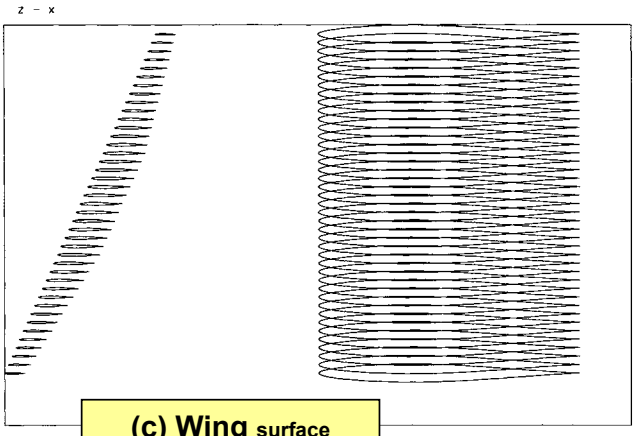

(c) Wing surface

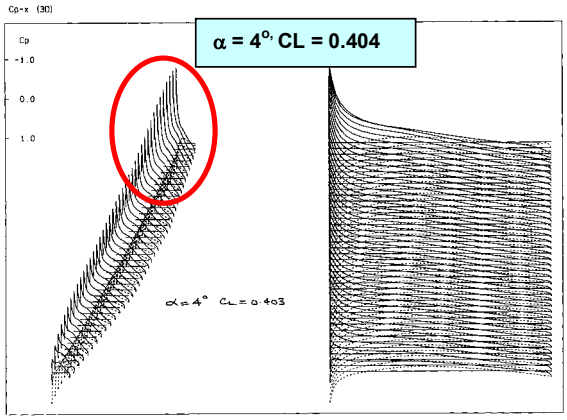

(d) Cp Distributions

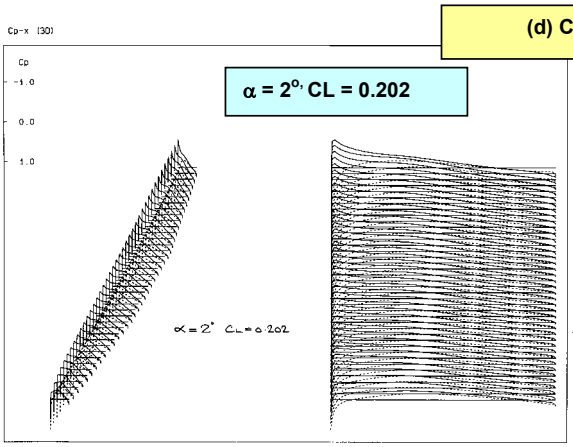

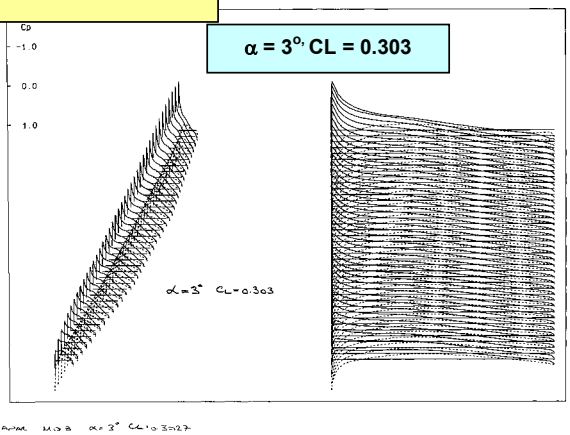

Fig. 7 30° OFW ISOLATED PLANAR CASE
Mach 0.8, AoA Effects

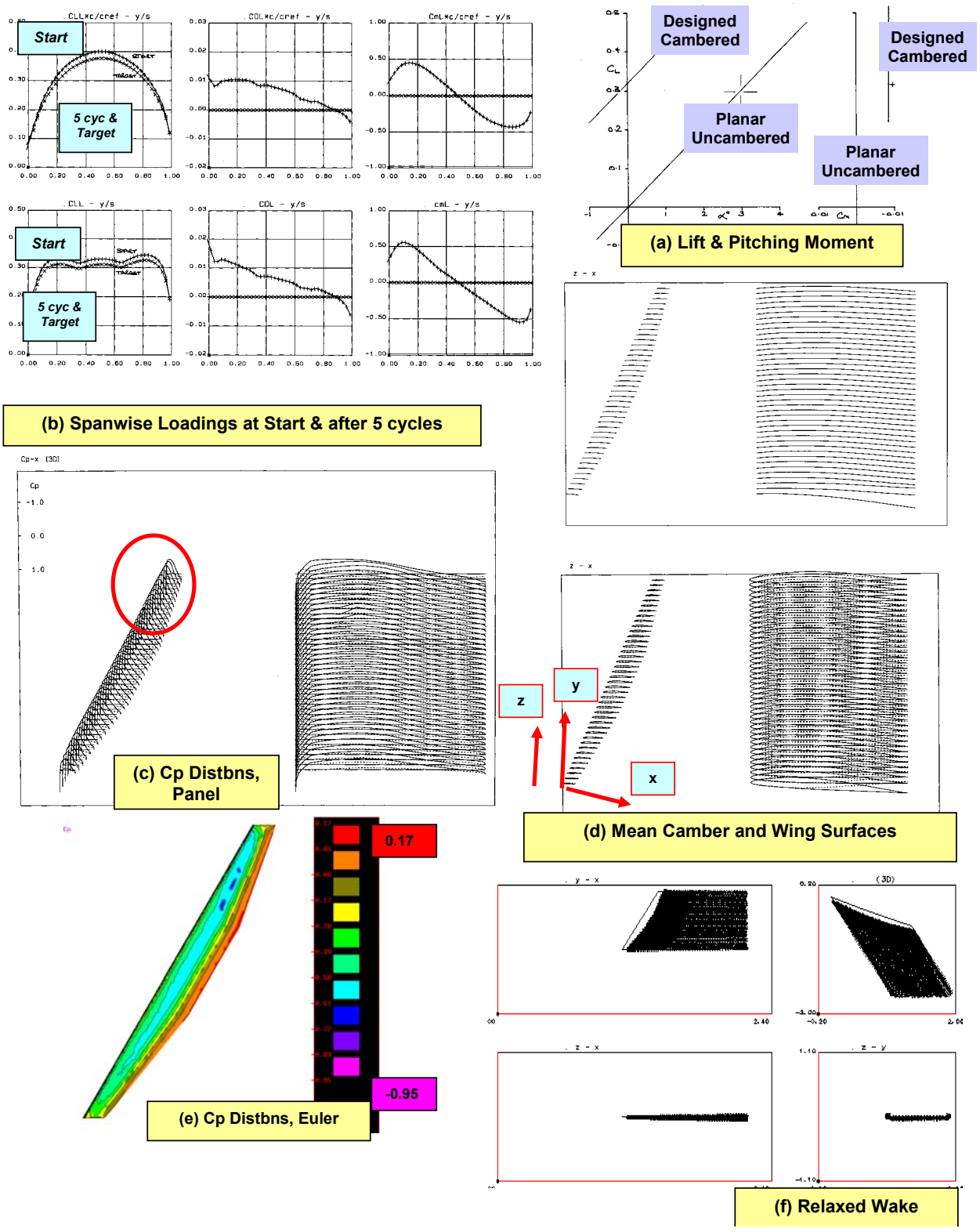

Fig. 8 30° OFW ISOLATED DESIGN CASE
No C_{LL} constraint, Mach 0.8, C_L=0.3

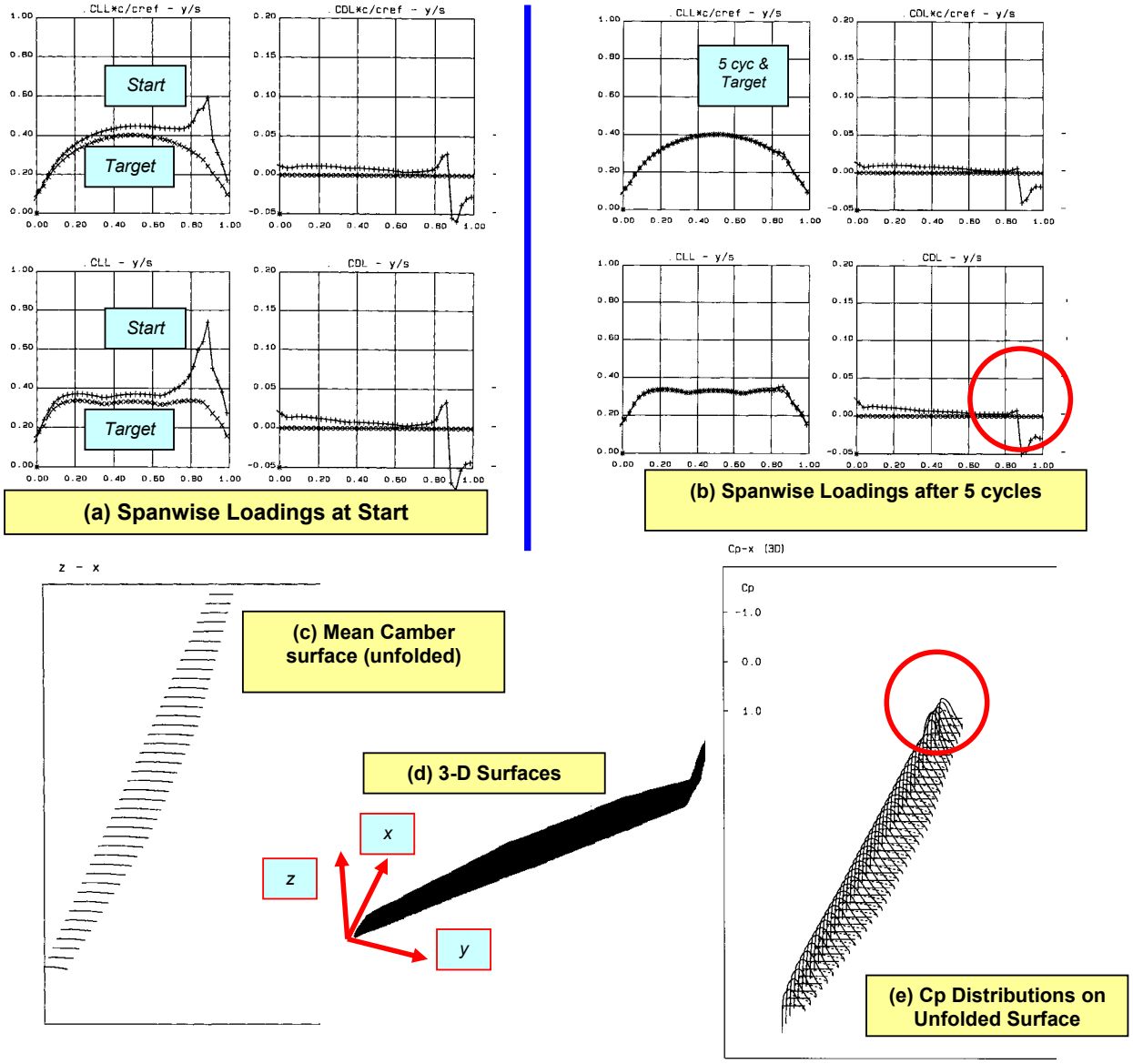

Fig. 9 30° OFW + 75° Folded-Tip / Winglet, No C_{LL} constraint, Mach 0.8, C_L = 0.3

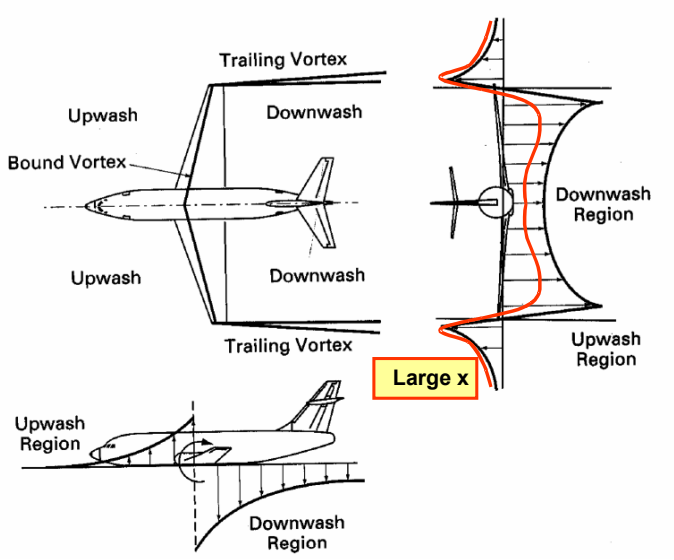

FIG. 10 WAKE EFFECTS

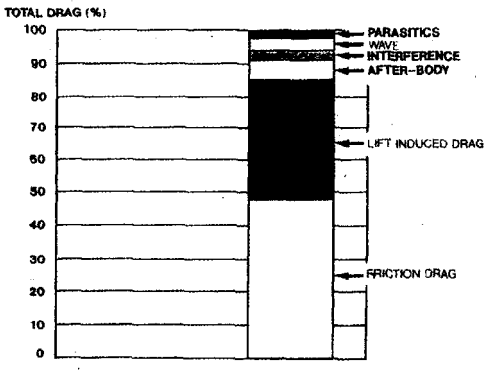

FIG. 11 Drag Breakdown of a Typical Aircraft (Ref.2)

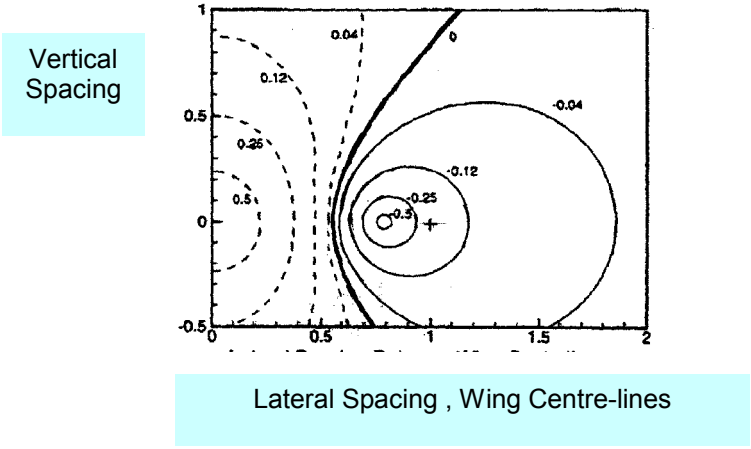

FIG. 12 Induced Drag as Function of Relative Position

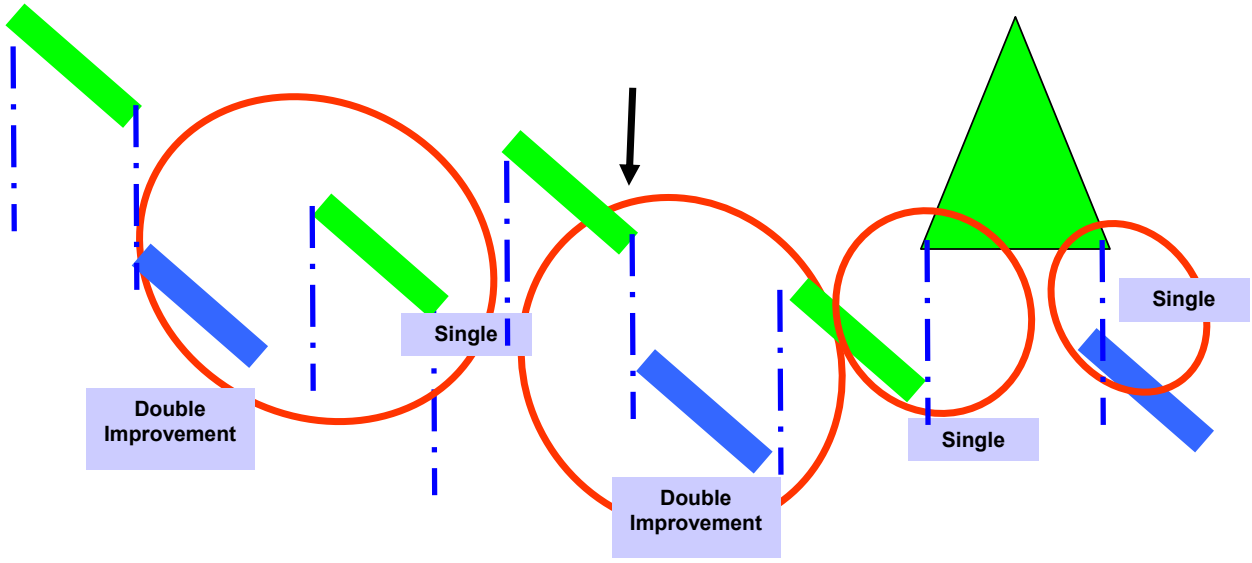

Fig. 13 OBLIQUE FLYING WINGS, SWARM

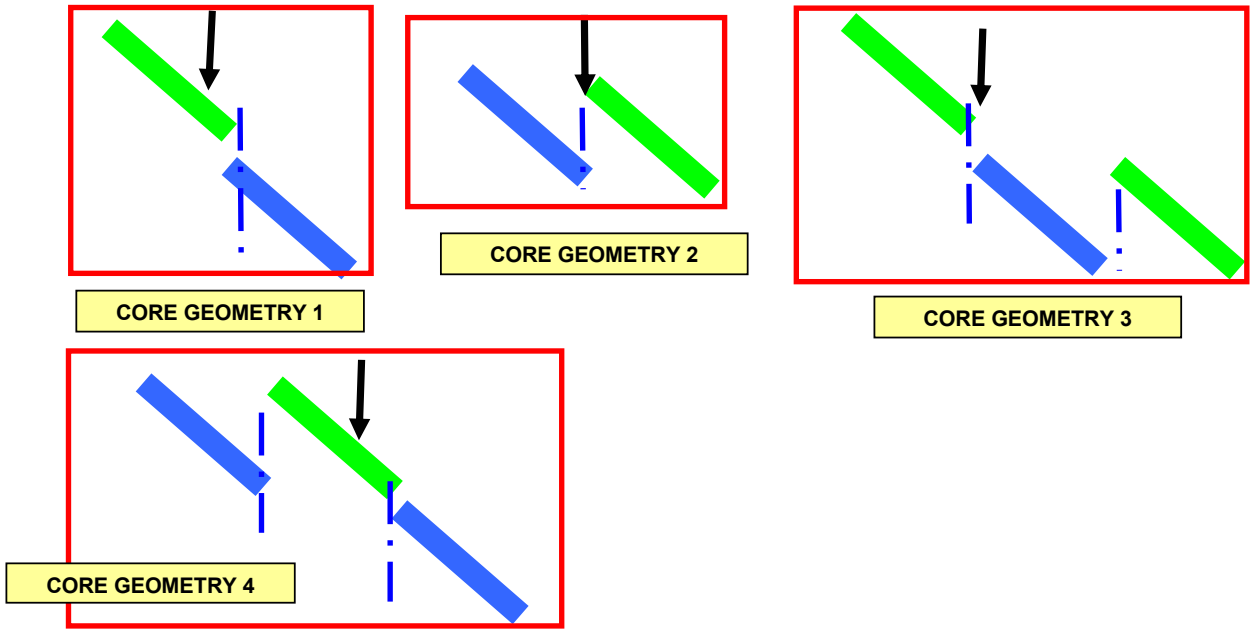

Fig. 14 OBLIQUE FLYING WINGS, CORE GEOMETRY TYPES

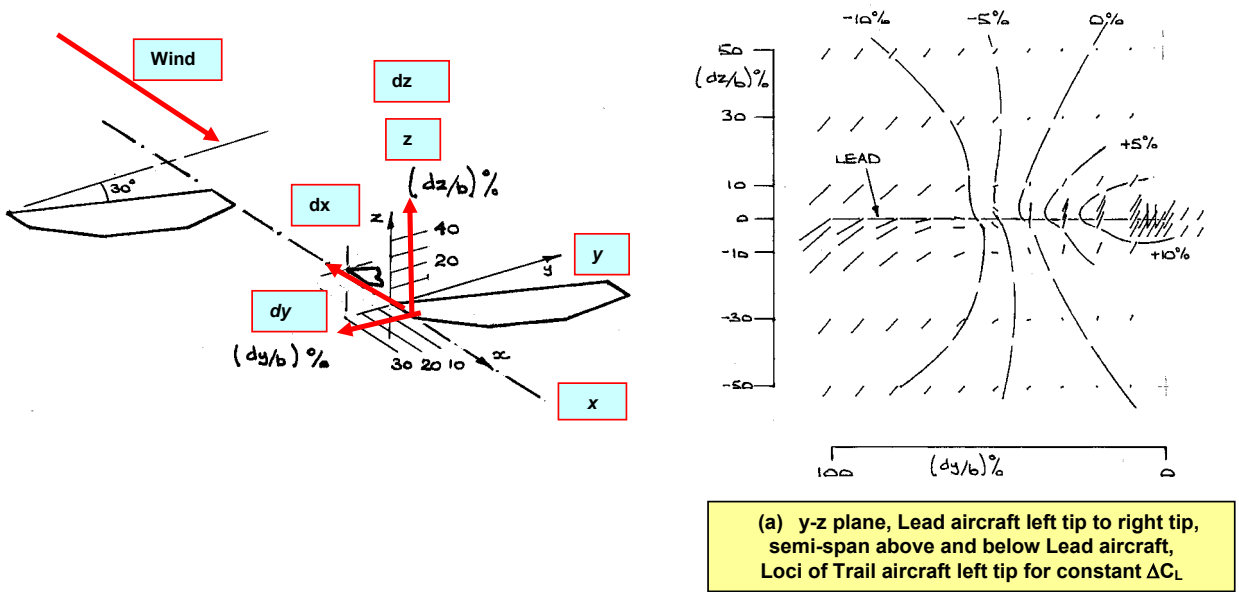

(a) y-z plane, Lead aircraft left tip to right tip, semi-span above and below Lead aircraft, Loci of Trail aircraft left tip for constant ΔC_L

Fig. 15 CORE 1 FORMATION DISPLACEMENTS, GEOMETRY DEFINITIONS

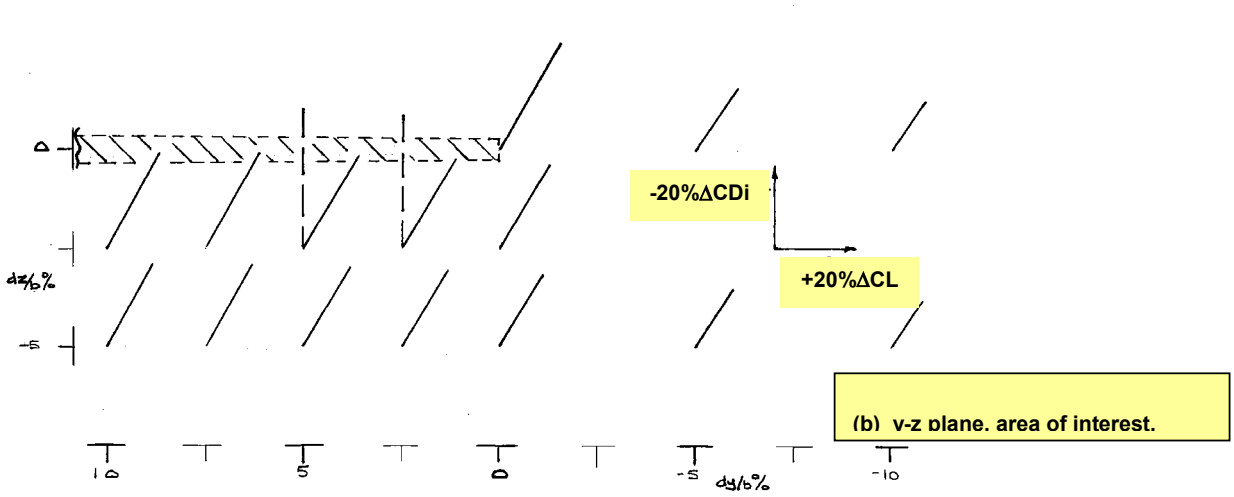

(b) v-z plane, area of interest.

Fig. 16 OFW CORE 1, CHANGES IN C_L and C_D EXPERIENCED BY TRAIL AIRCRAFT

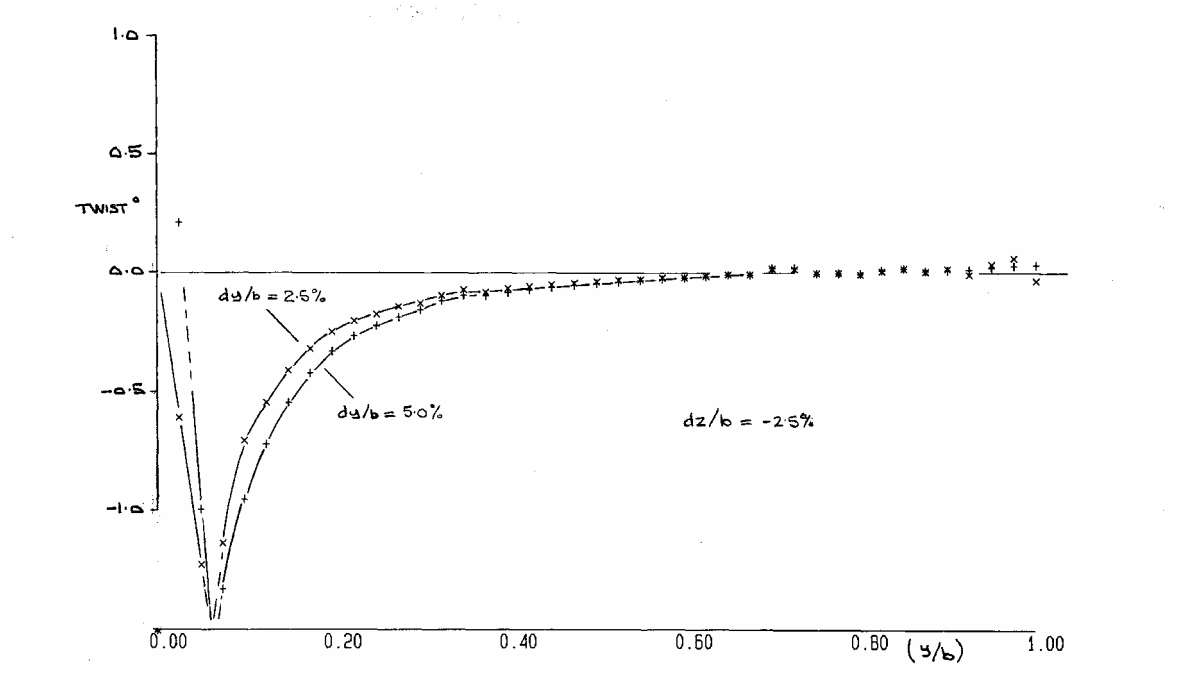

Fig. 17 TRAIL WING REDESIGNED FOR DESIGN C_L AND ZERO C_l IMPLIED TWIST INCREMENTS

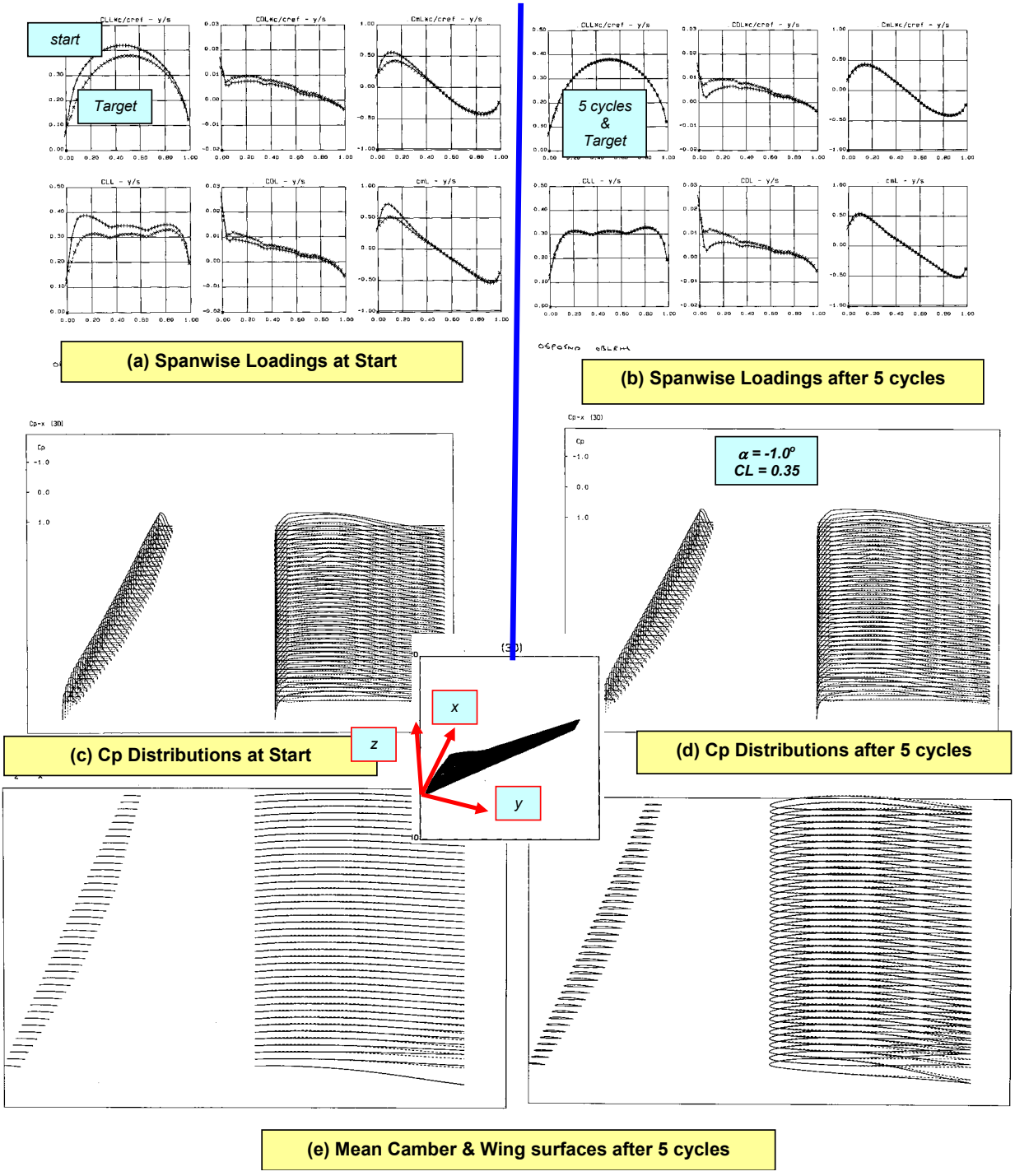

Fig. 18 FORMATION CORE GEOMETRY 1, 2.5% dy/b –2.5%dz/b DISPLACEMENT, RE-DESIGN TO ELIMINATE INDUCED EFFECTS, Mach 0.8, CL = 0.3

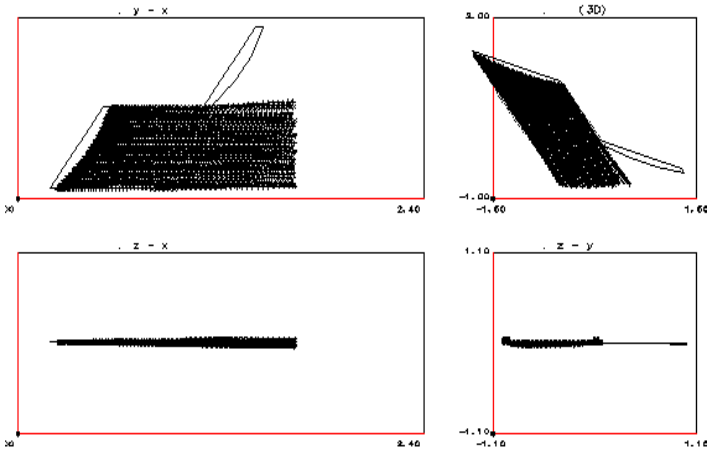

Fig. 19 FORMATION CORE 1 GEOMETRY, LEAD AIRCRAFT RELAXED TRAILING WAKE

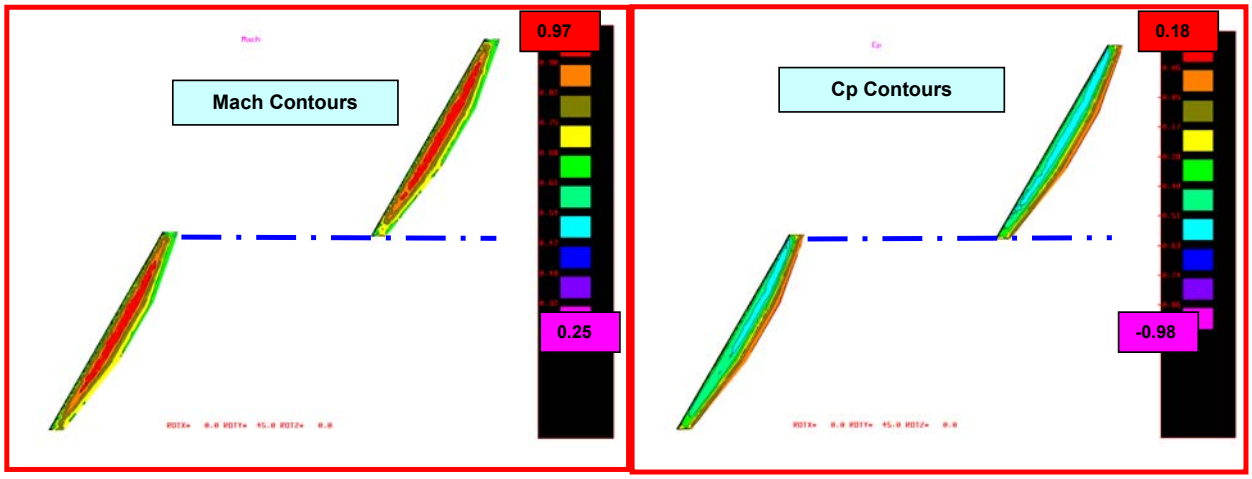

Fig. 20 CORE-1 FORMATION
MACH & Cp CONTOURS ON UPPER SURFACES, AT START

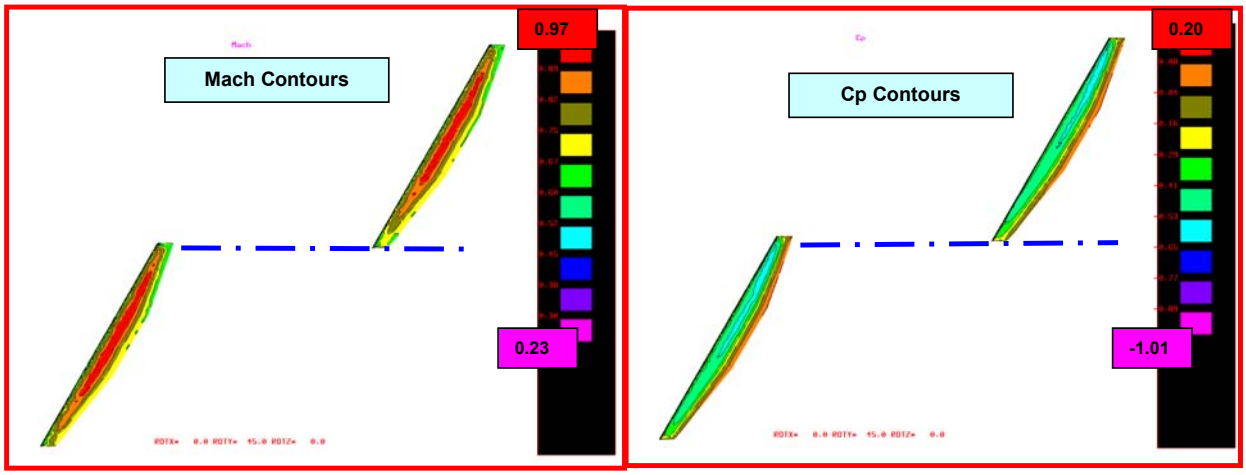

Fig. 21 CORE-1 FORMATION
MACH & CP CONTOURS ON UPPER SURFACES, AFTER CAMBER CONTROL

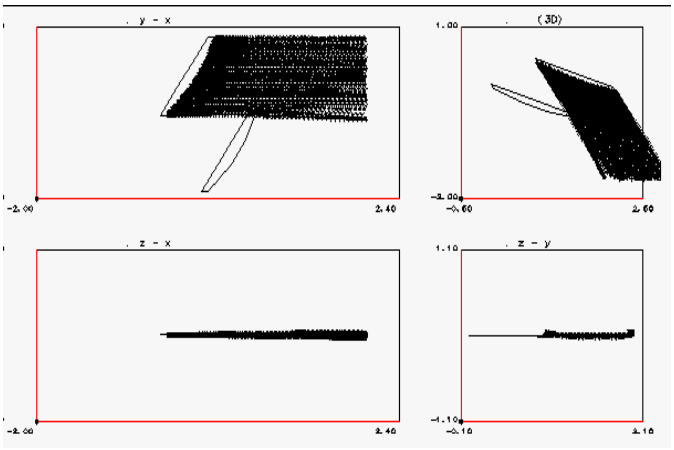

Fig. 22 FORMATION CORE 2 GEOMETRY, LEAD AIRCRAFT RELAXED TRAILING WAKE

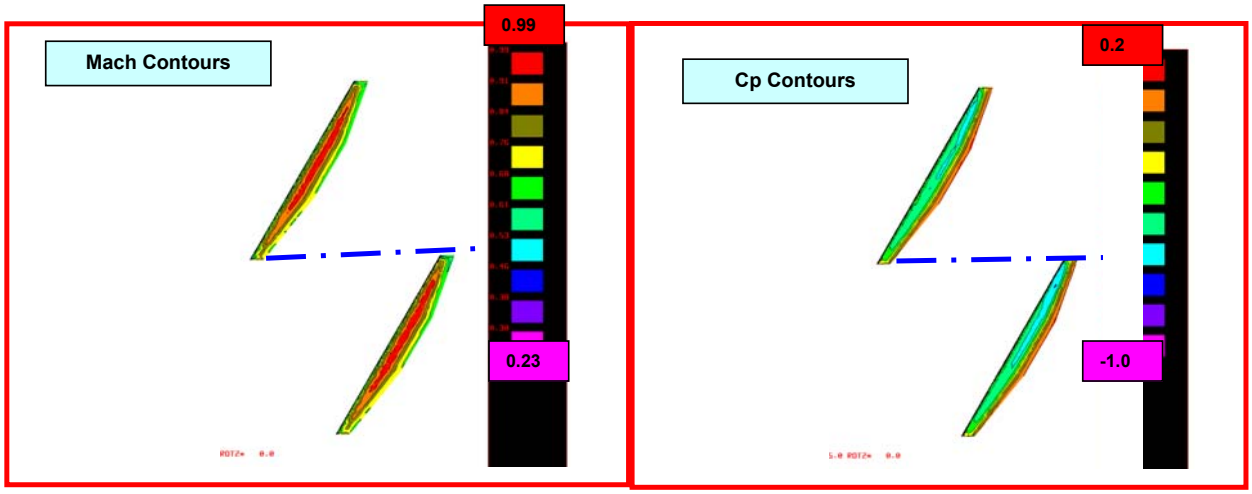

Fig. 23 CORE-2 FORMATION
MACH & Cp CONTOURS ON UPPER SURFACES, AT START

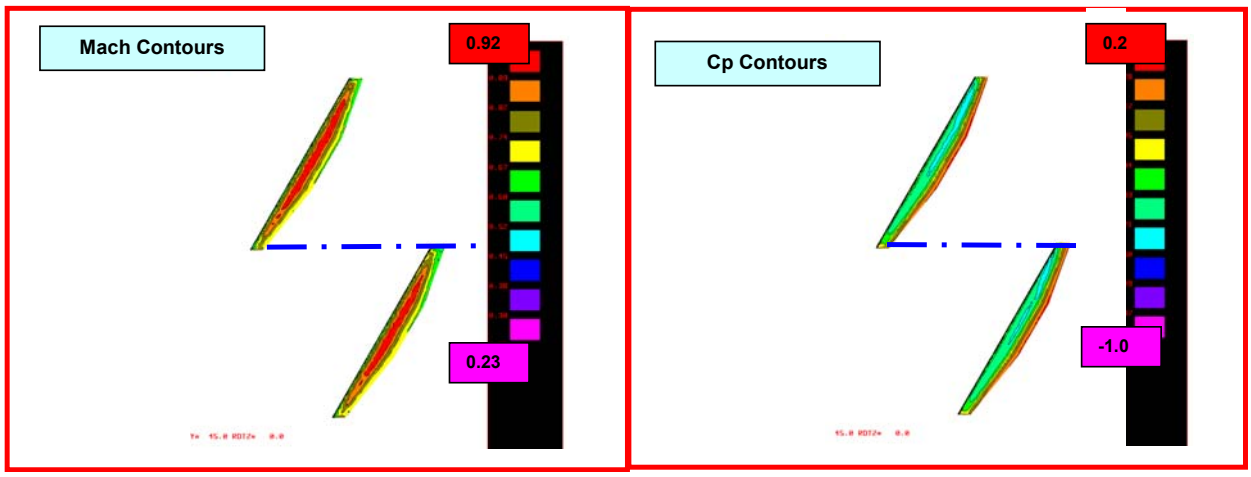

Fig. 24 CORE-2 FORMATION
MACH & CP CONTOURS ON UPPER SURFACES, AFTER CAMBER CONTROL

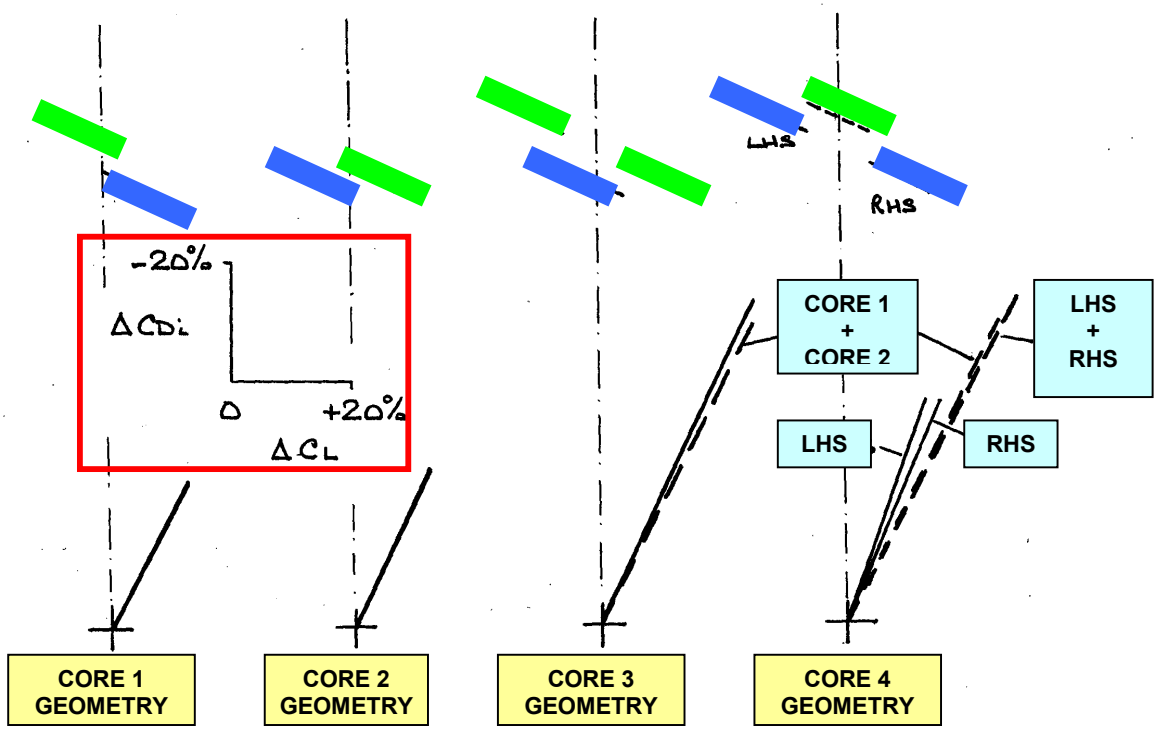

Fig. 25 CHANGES IN C_L and C_{Di} EXPERIENCED BY TRAIL AIRCRAFT
EXPRESSED AS % of ISOLATED AIRCRAFT C_L & C_{Did}
VARIOUS FORMATION GEOMETRIES, dy/b=0.0%, dz/b=-2.5%

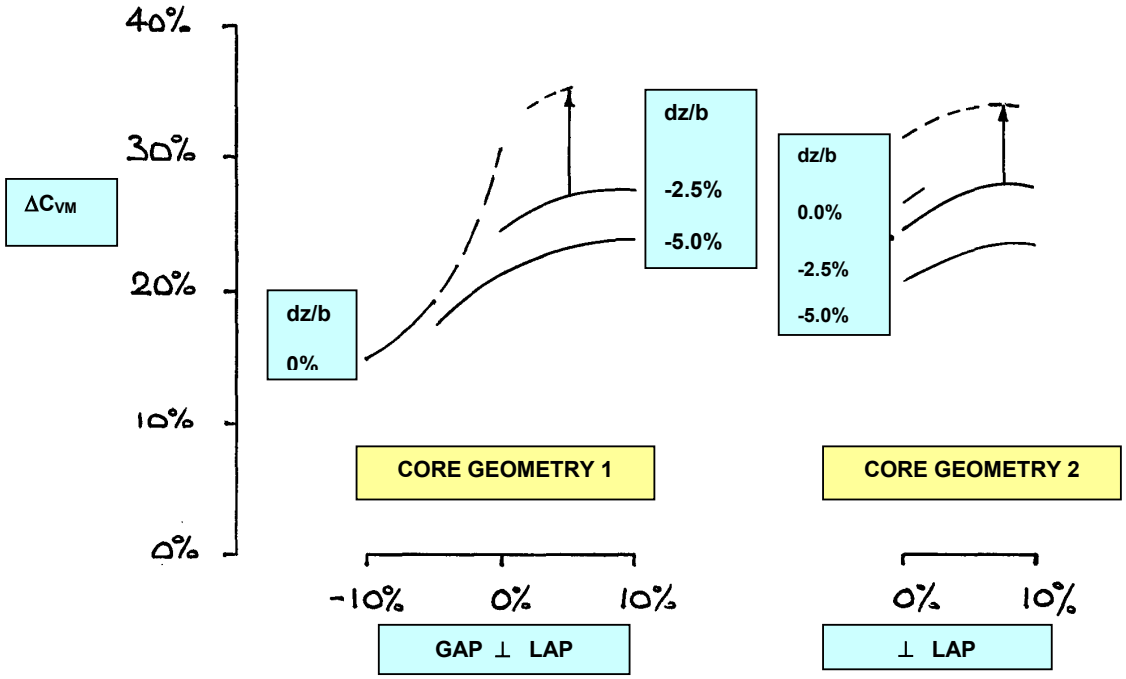

Fig. 26 TRAIL AIRCRAFT ΔC_{VM} and ΔC_{Di} VECTOR MAGNITUDE,
VARIATION WITH SPANWISE LOCATION,
EFFECT OF VERTICAL DISPLACEMENT, M=0.8

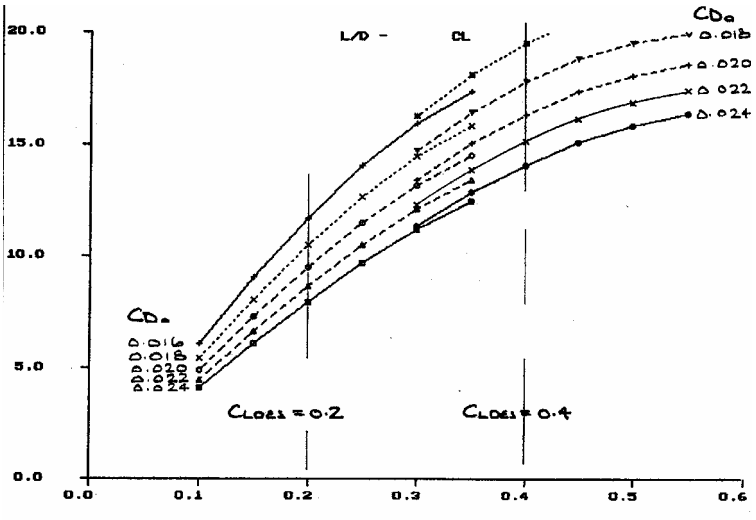

FIG. 27 L/D VARIATION WITH C_L

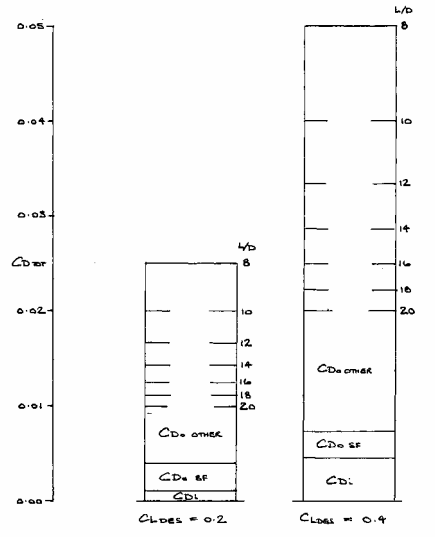

FIG. 28 TOTAL DRAG BREAKDOWN, C_{Di}, C_{DSF}, & C_{Dother} CONTRIBUTIONS FOR VARYING L/D AT Mach 0.8, CLdes = 0.2 & 0.4

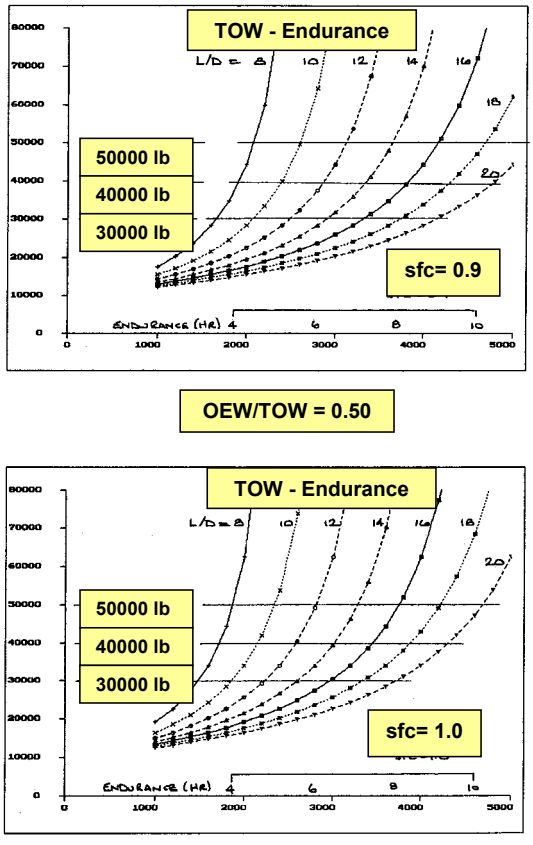

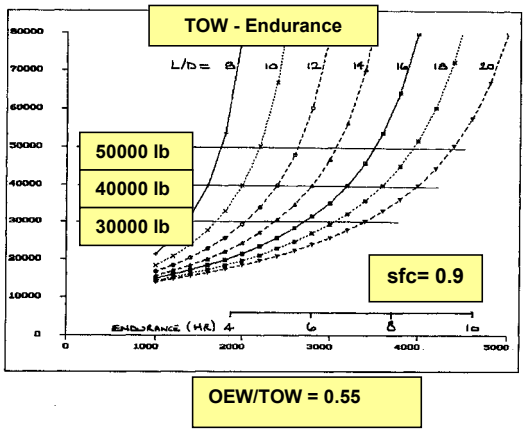

FIG. 29 TOW (lb) vs RANGE (nm) & ENDURANCE (hr), EFFECT OF L/D & sfc, OEW/TOW = 0.50, Mach 0.8

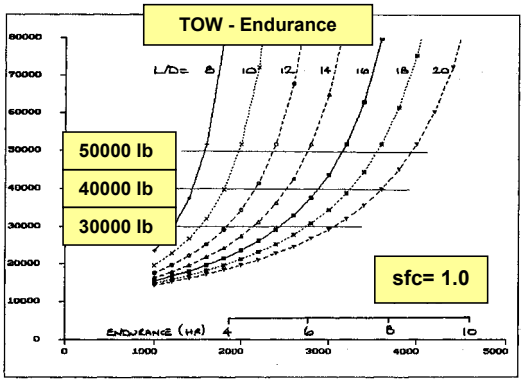

FIG. 30 TOW (lb) vs RANGE (nm) & ENDURANCE (hr), EFFECT OF L/D & sfc, OEW/TOW = 0.55, Mach 0.8